BIOCHEMICAL AND BIOPHYSICAL RESEARCH COMMUNICATIONS **247,** 154–158 (1998)
ARTICLE NO. RC988557

Ocular Lens NAD Kinase: Partial Purification and Metabolic Implications

Dana Young,* Michael Tallman,† Kathleen Landy,‡ Tara Young,§ David Lukas,¶ Barbara Lewis,‖ and Eugene McGuinness**,[1]

*UMDNJ, School of Dentistry, Newark, New Jersey 07103; †Unilever Research U.S., Inc., Englewood Cliffs, New Jersey 07020; ‡Reckitt & Colman, Inc., Montvale, New Jersey 07645; §UMDNJ, Graduate School of Biomedical Sciences, Newark, New Jersey 07103; ¶Schering-Plough Corp., Kenilworth, New Jersey 07033; ‖Givaudan Roure Corp., Clifton, New Jersey 07015; and **Department of Chemistry, Seton Hall University, South Orange, New Jersey 07079*

Received March 30, 1998

The ocular lens displays a significant amount of NADP(H) dependent metabolic traffic, but the origin of this cofactor has not been established. Size exclusion chromatography of bovine lens crude extract on a Sephacryl S300-HR column fitted with an eluate concentrator revealed two bands with NAD kinase activity, based on enzymatic cycling with signal amplification of the column fractions using a Cobas-Fara II centrifugal fast analyzer. V_e/V_o ratios from the chromatographic runs suggest that the relative molecular weight values lie within the ranges 8.91–3.98 $\times$ 10^5 and 2.04–1.26 $\times$ 10^5, respectively, for these two bands. An ~10-fold enhancement of enzyme activity over the crude fraction is realized from the chromatography step. Results point to NAD kinase as the source generator of this anchoring and linking cofactor for the oxidative stress and pentose phosphate enzyme systems, respectively.

The connecting link between the HMPP and oxidative stress (or glutathione redox cycle) enzyme systems is through the NADP-specific GR component of this cycle. With insufficient NADP(H) the coordinated reactions of these oxidative stress enzymes (GR, GPX) are severely diminished or rendered inoperative (1). The very high redox set point (GSH/GS-) associated with the ocular lens insures the quick recycling of GSSG back to GSH. This process uses an active GR coupled to a relatively large capacity to produce NADPH via the HMPP. Thus, it is really glucose that is supplying the reducing potential to the cell (2). Given the critical role of NADP(H) in these events, the question is raised, what is the origin of this cofactor in lens tissue?

NAD kinase (NADK, ATP:NAD 2′-phosphotransferase, EC 2.7.1.23) catalyzes the only known reaction leading to the production of $NADP^+$. This enzyme is widely distributed, and acknowledged to play a central role in the metabolism of many tissues (3). Its presence in rat brain (4), pigeon retina (5) and monkey retina (6) has been demonstrated. The origin of NADP(H) in the ocular lens has not been previously established. Here we report the results of our investigation on the presence of NADK in lens tissue using a combination of column eluate concentration chromatography and enzymatic amplification on a centrifugal fast analyzer.

MATERIALS

The chemicals (suppliers) used in these experiments were as follows: NH_4OAc, EDTA, Na_2 salt, $K_2Cr_4O_7$, SDS, and H_2SO_4 (Fisher Scientific Co., Fair Lawn, NJ 07410); H_2O_2 (30%, Clean-room Grade, Ashland Chemical Co. procured from Brand-Nu Laboratories, Meriden, CT 06450). Fresh frozen bovine whole eyeballs were obtained from the Pel-Freeze Corp., Conway AR 72757.

NADK (Type IV, chicken liver,), G6PDH (Type IX, Baker's yeast), GLUDH (Type III, bovine liver), 6PGDH (sheep liver), and DTE were purchased from Sigma Chemical Co., St. Louis, MO 63178. Catalase (*Aspergillus niger*) was supplied by Calbiochem-Behring Corp., La Jolla, CA 92037. The Bradford protein assay reagent was acquired from Bio-Rad Laboratories (Richmond, CA 94804). Sephacryl S300HR was obtained from Pharmacia Biotech, Piscataway, NJ 08854. Unless otherwise noted all additional reagents, chemicals and enzymes were procured from Sigma.

[1] Corresponding author: Department of Chemistry, Seton Hall University, So. Orange, NJ 07079. Fax: (973) 761-9772. E-mail: mcguineu@shu.edu.

The abbreviations used are: ADP, adenosine 5′-diphosphate; ATP, adenosine 5′-triphosphate; BSA, bovine serum albumin; CEC, column eluate concentrator; CFA, centrifugal fast analyzer; DTE, dithioerythritol; EDTA, ethylenediamine tetraacetate; GLU, L-glutamate; GLUDH, L-glutamic dehydrogenase; G6P, glucose 6-phosphate; G6PDH, glucose 6-phosphate dehydrogenase; GSH/GSSG, GS^-, glutathione, reduced/oxidized; GPX, glutathione (GSH) peroxidase; GR, glutathione (GSSG) redutase; HMPP, hexose monophosphate pathway; α-KG, α-ketoglutarate; NAD(H), β-nicotin-amide adenine dinucleotide; NADK, nicotinamide adenine dinucleotide kinase; NADP(H), β-nicotinamide adenine dinucleotide phosphate; PFK, phosphofructokinase; 6PG, 6-phospho-gluconate; 6PGDH, 6-phosphogluconic dehydrogenase; PMSF, phenylmethyl sulfonyl fluoride; Ru5-P, ribulose 5-phosphate; SEC, size exclusion chromatography; TCEP, tris(2-carboxy-ethyl)phosphine; TRIS(HCl), tris(hydroxymethyl) aminomethane (hydrochloride).

0006-291X/98 $25.00

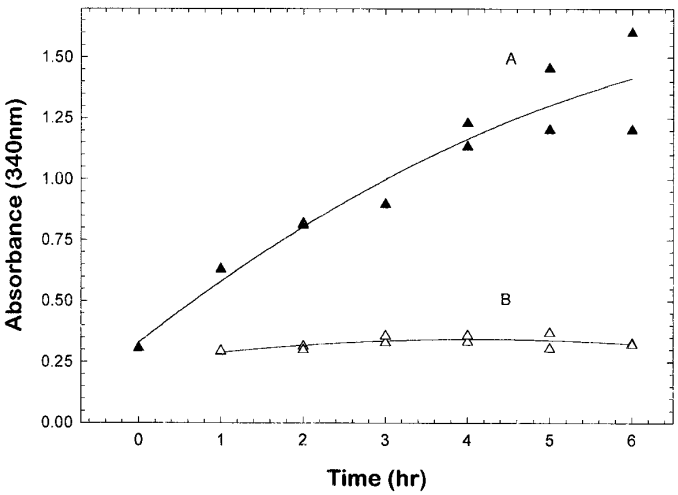

FIG. 1. Amplified stop-time activity plots generated by the addition of crude extract, prepared from anterior slices of bovine lens, to reaction mixtures containing NAD^+ and ATP/Mg^{++} (A) or NADH and ATP/Mg^{++} (B).

METHODS

Hydrogen Peroxide Measurement

H_2O_2 concentrations were determined from absorbance measurements at 240 nm (7) or by the TCEP method of Han *et al.* (8).

Protein Assay

Protein measurements were based upon the Coomassie blue G-250 dye method (9), as furnished by Bio-Rad Laboratories (Richmond, CA, 94804). BSA was used as the protein standard.

Crude Extract Preparation

All operations were carried out in an ice, water and salt bath to hold the temperature below 4°C. Thin latitudinal slices of varying thicknesses (~0.1-0.4mm) were taken from different regions (e.g., polar, equatorial) of the anterior and posterior sections of the decapsulated ocular lens. Within a given experiment all slices were excised from the same location using ~10-15 lenses removed from whole, frozen eyeballs. The majority of experiments were performed on sections excised from the anterior hemisphere.

Each slice of lens tissue was hand homogenized (glass homogenizer) in 50 mM TRIS-HCl buffer (pH 7.4) containing EDTA (20mM), DTE(5.0mM) and PMSF (0.5 mM). The crude extract was then centrifuged at 17×10^3g (60 min). If necessary, an additional centrifugation was carried out to insure total clarity of the supernatant. The clear supernatant was decanted, stored in (1.0 mL) plastic vials and frozen (−20°C).

Size Exclusion Chromatography

Aliquots (~1-5 mL) of the stored, clear crude extract were taken to 4°C and placed on a gel column (1.3 cm × 90 cm or 2.5 cm × 38 cm) of Sephacryl S300HR fitted with a column eluate concentrator (Amicon Model 530, Millipore Corp., Bedford, MA 01730) equipped with a YM10 ultrafilter membrane. Sample fractionation was carried out using the crude-extract buffer as eluting solvent at a flow rate of ~50-60 mL/hr and CEC settings adjusted to provide between 1.5→5 fold concentration. These operations were performed on a low-pressure liquid chromatographic system (Model 731-8101, Bio-Rad Laboratories, Hercules, CA 94547).

Enzymatic Assays

NAD kinase activity measurements were carried out (37°C) in a 2-step process using (i) a discrete stop-time assay for each sample [Eqn. 1], followed by (ii) enzymatic amplification and indicator-reaction readout. The amplification [Eqns. 2, 3] and reaction readout steps [Eqn. 4] were performed as a continuous operation using 30-position disposable cuvettes on a Cobas-Fara II® CFA (Roche Diagnostic Systems, Somerville, NJ 08876).

$$ATP + NAD^+ \longrightarrow ADP + NADP^+ \quad [1]$$

$$G6-P \longrightarrow 6PG \quad [2]$$

$$NADP^+ \quad NADPH/H^+$$

$$H_2O + GLU \longleftarrow a-KG + NH_4^+ \quad [3]$$

$$NADP^+ + 6PG \longrightarrow Ru5\text{-}P + CO_2 + NADPH/H^+ \quad [4]$$

(i) The NADK stop-time reaction. Each reaction [Eqn. 1] was initiated by the addition of an aliquot of crude extract (0.1-0.4 mL; 0.1-0.5 mg protein/10mL), allowed to run for a variable but preset time (~10min-6hr) and terminated by placing the individual reaction vessels in a boiling water bath for 3 min. All samples were then centrifuged (~4° C, $14*10^3$g, 15 min) to remove denatured protein and stored at 0-4° C. Aliquots from these samples were subsequently amplified and read out as described below.

(ii) Enzymatic amplification. The strategy invoked to perform a continuous enzymatic amplification reaction on the CFA makes use of three discrete transfer steps (T1-T3) during the course of the multi-sample (~25-28) run. These involve a sample transfer to cycle-reagent step, followed by cycle initiation and amplification in one continuous operation (T1). Cycle termination is achieved by addition of a kill-reagent to the cycled sample mixture (T2). This, in turn, is followed by transfer of the indicator reagent to the terminated reaction mixture, containing the amplified sample, cycle-reagent and kill-reagent, for absorbance readout at 340 nm (T3). Cycle specificity is dictated by the ($NADP^+$-dependent) G6PDH reaction [Eqn. 2].

$NADP^+$ standards used to generate the amplification-step calibration curve were carried through each run and subjected to the same treatment as the samples. Detailed protocols for the preparation of reagents, samples, standards and instrument settings, diagnostic plot interpretations and calculations, as they relate to the CFA, are given elsewhere (10, 11). Data analysis was performed using SigmaPlot and SigmaStat (SPSS Inc., Chicago, IL 60611). Enzyme activity values as reported (picomoles/mg and picomoles/hr/mg), are corrected for amplification.

RESULTS

When NAD^+ and ATP/Mg^{++} were incubated with crude extract in a series of stop-time assays over a 1-6 hr time span, plot pattern A (Fig. 1, upper curve) was generated. The amplified activity vs time curve suggests that the crude extract incubation mixture is stable for about 1.5 - 2 hrs at 37° C before activity begins to level off. In contrast, when the NAD^+ in these runs is replaced with NADH as reactant, plot pattern B (Fig. 1, lower curve) is generated. Clearly, the ab-

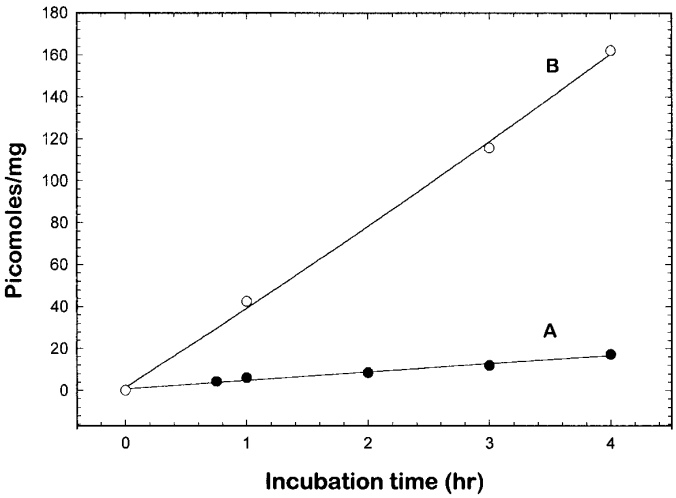

FIG. 2. Stop-time activity plots generated by the addition of NAD^+ and ATP/Mg^{++} to lyophilized preparations of: (A) crude extract and (B) chromatographic eluant from a crude extract fraction. Protein concentrations and amplification factors were: (A) 66.4 mg/mL, 813; (B) 11.6 mg/mL, 3.688. Specific activities corresponding to the 0.75 → 4 hr time increments are: (A) 5.6, 6.0, 4.3, 3.9, and 4.3; (B) 42.4, 38.6, and 40.5 picomoles/hr/mg, respectively.

sorbance change produced by the crude extract in plot A is NAD^+-dependent. The presence of NADH elicits no enzymic response.

When NAD^+ and ATP/Mg^{++} were incubated with a crude extract that was lyophilized immediately following preparation, stored frozen and subsequently reconstituted with distilled water, the resulting plot pattern (Fig. 2A) suggests that enzyme activity remains stable over a ~0-4 hr time span. Another portion of this same crude extract was subjected to Sephacryl S300HR chromatography immediately following preparation, then lyophylized and stored frozen. When subsequently reconstituted with distilled water, the stop-time vs activity curve generated by this preparation (Fig. 2B) exhibited a marked increase in enzyme activity relative to the lyophilized crude extract (Fig. 2A). A comparison of activities (B/A ratios) at the 3rd and 4th hr points to a ~9-10 fold increase (i.e., 9.8, 9.4) in activity following this SEC step.

Subsequent SEC fractionation of a crude extract preparation revealed the presence of two bands of enzyme activity (Fig. 3, Bα, bands 1 and 3) in a ratio of ~2.2 (i.e., 11.6/5.3). This experiment was repeated, but without added NAD^+ (Fig. 3, Bβ). The lack of significant activity above background across these fractions is indicative of the fact that lens crystallins-sequestered NADP(H) (12) is removed by the SEC step on Sephacryl S300HR. Were it retained, we would anticipate higher levels of background activity, since the in-situ cofactor would be amplified in both the Bα and Bβ experiments.

Inclusion of the decapsulated epithelial layer in a thin-slice anterior-section crude extract preparation subjected to SEC gives rise to a significant increase in activity (Fig. 4, bands 2, 4). It is noteworthy that the major/minor activity band ratios in this and the previous run (Fig. 3Bα are of similar magnitude at 2.6 (136.4/53.5) and 2.2 (11.4/5.1), respectively. In addition, a comparison of the counterpart major and minor activity bands from the separate experiments to each other reveals that these ratios are also of similar magnitude at 12.0 (136.4/11.4) and 10.5 (53.5/5.1), respectively.

Given the between-run variations in flow rate, chart speed and concentration ratios for the individual SEC experiments, a comparison by fraction numbers does not provide a useful basis for evaluation between different experiments. For example, the major enzyme activity bands appear to occur in the 1st and 3rd fractions in one case (Fig. 3), and the 2nd and 4th fractions in the other (Fig. 4).

If, however, comparison based on the reciprocal of the retention coefficients (V_e/V_o ratios) is made, the discrete bands of activity are seen to fall within the

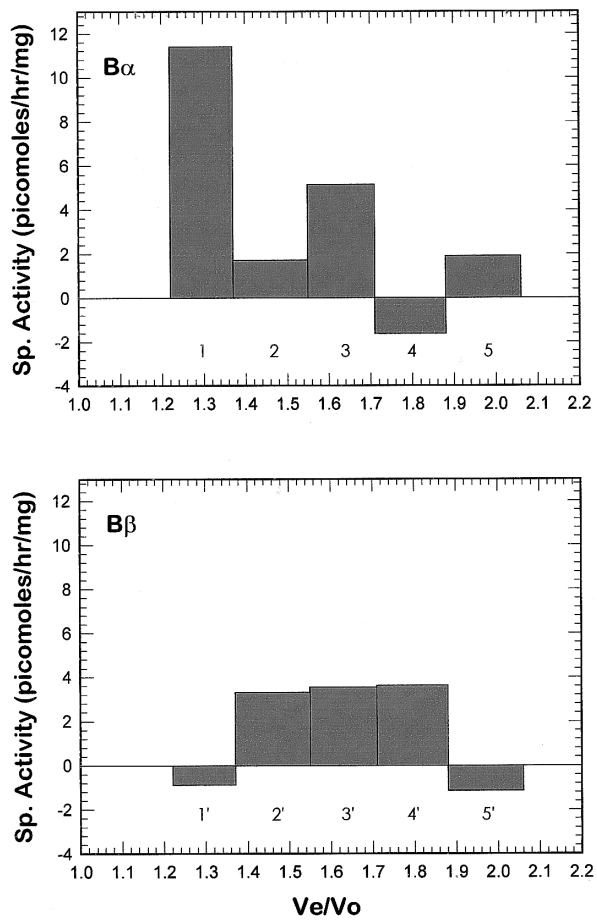

FIG. 3. Specific activity patterns of five effluent fractions of crude extract derived from an anterior section of bovine lens following SEC on Sephacryl S300HR. (Bα) Run in the presence of added NAD^+ and ATP/Mg^{++}. (Bβ) Run in the absence of added NAD^+.

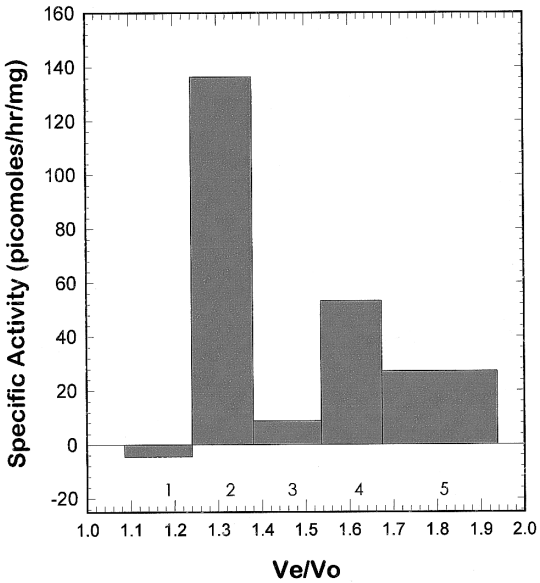

FIG. 4. A rerun of the experimental conditions described for Fig. 3Bα, but with the crude extract taken from a thin anterior section including the epithelial layer.

ranges 1.22-1.38 and 1.54-1.71 in both experiments (Table 1). These V_e/V_o ratios translate into molecular weight range estimates of $\sim$8.91-3.98 $\times 10^3$ and $\sim$2.04-1.26 $\times 10^3$, respectively. Such size estimates would place these activities within the α- and β_H- crystallin fractions of the ocular lens, based on calibration runs using proteins of known molecular weights with Sephacryl S300HR.

DISCUSSION

The NAD kinase enzyme activity profile that emerges from measurements across latitudinal sections of the decapsulated ocular lens in this investigation reveals that the highest activity is localized in the anterior polar region of the epithelial layer, with diminishing to trace amounts found as we move posteriorly to the equatorial region. Similarly, the anterior capsulolenticular layer and the posterior polar regions exhibited only trace amounts of activity. This pattern of NADK activity mirrors the collective assessment of previous histochemical studies where the most intense staining for lens enzymes was always found in the epithelium, and decreased towards the nucleus (13).

The evidence for multiple bands of NAD kinase activity in bovine lens is in accord with previous studies from other sources which indicate this enzyme is a large multimeric complex (14). Recently Filippovich et al., (15) have identified 10 molecular forms of NADK in the Colorado potato beetle with M_r values ranging from $80*10^3$ to $1.0*10^6$. Pou de Crescenzo et al., (16) established the existence of 5 forms of NADK of comparable specific activity, isolated from asynchronous cultures of the achlorophyllous ZC mutant of *Euglena*

TABLE 1

Data Comparison from Separate Experiments of Different Anterior Section Slices of Bovine Ocular Lens, Showing the Locus of Molecular Weights Relative to the Specific Activity, Based on V_e/V_o Ratios

	Volumes				Molecular weight ranges			
Fraction #	V_t mL	V_c Δ mL	V_t/V_c Ratio	V_e/V_o Ratio	Log Values	$\times 10^3$ High	$\times 10^3$ Low	Specific activity pmol/hr/mg
				Expt #24				
0	16.36	7.21	2.27					
1	14.25	6.33	2.25	1.22–1.37	5.95–5.61	891	398	11.4
2	14.26	6.33	2.25	1.37–1.55	5.61–5.41	398	204	1.7
3	12.76	5.66	2.25	1.55–1.71	5.41–5.03	204	141	5.1
4	14.26	6.28	2.27	1.71–1.88	5.03–4.70	141	50	1.6
5	14.84	6.59	2.25	1.88–2.06	4.70–4.42	50	27	1.9
Σ	86.73	38.40	2.26					
				Expt #27				
0	10.50	6.33	1.66					
1	14.90	9.03	1.65	1.09–1.24	6.18–5.87	1514	741	−4.3
2	13.50	8.13	1.66	1.24–1.38	5.87–5.60	741	398	136.4
3	15.00	9.04	1.66	1.38–1.54	5.60–5.31	398	204	8.9
4	13.50	8.13	1.66	1.54–1.67	5.31–5.10	204	126	53.5
5	25.50	15.36	1.66	1.67–1.94	5.10–4.59	126	39	27.2
Σ	92.90	56.02	1.66					

Note. The volume descriptors refer to the total (V_t), concentrated (V_c), elution (V_e) and void (V_o) volumes, respectively. The Σ values designate the summed fraction volumes (0–5) and mean V_t/V_c ratios.

gracilis. These forms, characterized by M_r values of 40, 90, 170, 350 and >500 kDa when subjected to Sephacryl S-300 SEC, are suggested to consist of one polymeric native form (350 kDa, composed of 40 kDa subunits), and dissociated forms (170 and 90 kDa) of the native enzyme.

The location of the major band of NADK activity in the SEC elution profile corresponds to that found for ocular lens PFK (17). This enzyme, a tetramer with a molecular weight of $\sim 4*10^5$ and one of the largest enzymes in the lens, was found to elute in the α-crystallin fraction. Of the two interconvertible forms of lens PFK (I and II), PFK-II is believed to be the functional form because of its extreme sensitivity to numerous metabolic inhibitors and activators. In our studies the lower band of NADK activity appeared within the β_H fraction where, it was noted, most other enzymes elute (17).

Several aspects of the NAD^+, NADH, NADPH and $NADP^+$ concentration patterns found in bovine lens epithelium (1109, 202, 224 and 177 nmol/g wet wt, respectively (18)), may be of particular significance relative to our study. Since the NADPH/$NADP^+$ ratio ($\sim$1.3) is close to unity, this redox system is optimized to respond rapidly and simultaneously to the competing needs of the HMPP (for $NADP^+$) and GR (for NADPH). Given a rapid response capability and the very high level of NAD^+, we suggest that NADK-driven phosphorylation of NAD^+ may be initiated by any of its numerous and putative (or as yet unknown) effectors (19), called into play to rectify a transient NADPH/$NADP^+$ imbalance. It seems counterintuitive that epithelial aldose reductase, alone (18) or as part of the sorbitol (polyol) pathway (13), would function as the vehicle for oxidizing NADPH to keep the pentose phosphate pathway operating. Heavy traffic on this route could deprive GR of NADPH and also tend to generate a cataractogenic level of sorbitol (20).

Cofactor deprivation of GR may have additional negative consequences. For example, the increase in protein-GSH mixed disulfide (PSSG) that accompanies the loss of GSH in chronic H_2O_2 induced cataract in cultured rat lens was dethiolated spontaneously in the absence of hydrogen peroxide. It was suggested this dethiolation process of thioltransferase (TTase) requires GR and GSH and may play an important role in protecting other lens enzymes and proteins from oxidative damage (21). Reductive cleavage of mixed disulfides in intact cells involves both NADH- and NADPH-dependent processes (22). Ensuring that levels of ATP and NADPH are maintained subsequent to induced oxidative stress appears to be an important antioxidant response (23). It may be that, analogous to PFK, NADK lies at the nexus of a critical metabolic control point; in this case maintenance of the optimized ratios for [NADPH]/{$NADP^+$] and [NAD^+]/[$NADP^+$] unique to each cell.

ACKNOWLEDGMENTS

This work was supported by Grant EY0910-01A1 of the National Eye Institute of the National Institutes of Health and Roche Diagnostics Systems, Inc.

REFERENCES

1. Schirmer, H. R., Müller, J. G., and Krauth-Siegel, R. L. (1995) *Angew. Chem. Int. Ed. Engl.* **34,** 141–154.
2. Spector, A. (1995) *FASEB J.* **9,** 1173–1182.
3. McGuinness, E. T., and Butler, J. R. (1985) *Intl. J. Biochem.* **17,** 1–11.
4. Fernandes, M. (1970) *J. Neurochem.* **17,** 503–509.
5. Zhuchikhina, A. A., and Etingof, R. N. (1973) *Dokl. Acad. Nauk SSSR.* **212**(4), 996–999.
6. Berger, S. J., and DeVries, G. W. (1982) *J. Neurochem.* **38,** 821–826.
7. Bielski, B. H. J., and Allen, A. O. (1977) *J. Phys. Chem.* **81,** 1048–1050.
8. Han, J., Yen, S., Han, G., and Han, P. (1996) *Anal. Biochem.* **234,** 107–109.
9. Bradford, M. M. (1976) *Anal. Biochem.* **72,** 248–254.
10. Lewis, B. L., and McGuinness, E. T. (1990) *Anal. Biochem.* **184,** 104–110.
11. Eisenwiener, H-G., and Keller, M. (1979) *Clin. Chem.* **25,** 117–121.
12. Wistow, G. (1993) *Trends in Biochem. Sci.* **18,** 301–306.
13. Hockwin, O., and Ohrloff, C. (1981) *in* Molecular and Cellular Biology of the Eye Lens (Bloemendal, H., Ed.), pp. 317–413, Wiley, New York.
14. Butler, J. R., and McGuinness, E. T. (1982) *Int. J. Biochem.* **14,** 839–844.
15. Filippovich, S. Yu., Afanasieva, T. P., Olysevich, A. V., Bachurina, G. P., and Kritsky, M. S. (1996) *Comp. Biochem. Physiol.* **114B,** 251–256.
16. Pou de Crescenzo, M-A., Goto, K., Carre, I. A., and Laval-Martin, D. L. (1997) *Z. Naturforsch* **52c,** 623–635.
17. Cheng, H. M., and Chylack, L. T. (1985) *in* The Ocular Lens: Structure, Function and Pathology (Maisel, H., Ed.), pp. 223–264, Dekker, New York.
18. Giblin, F. J., and Reddy, V. N. (1980) *Exp. Eye Res.* **31,** 601–609.
19. Corimer, M. J., Harmon, A., and Putnam-Evans, C. (1985) *in* Calmodulin Antagonists and Cellular Physiology (Hidaka, H., and Hartshorne, D. J., Eds.), pp. 445–456. Academic Press, San Diego.
20. Yoshioka, S., Kameyama, K., Sanaka, M., Sekine, I., Kagimoto, S., Fujitsuka, S., and Saitoh, S. (1991) *Clin. Chem.* **37**(5), 686–689.
21. Wang, G.-M., Raghavachari, N., and Lou, M. F. (1997) *Exp. Eye Res.* **64,** 691–700.
22. Cotgreave, I. A., and Gerdes, R. G. (1998) *Biochem. Biophys. Res. Comm.* **242,** 1–9.
23. Agius, D. R., Bannister, W. H., and Balzan, R. (1998) *Biochem. and Molec. Biol. Intl.* **44**(1), 41–49.